

NGS-MUTATIONAL ANALYSIS OF DRIVER GENES AND TGFB1 WITH TUMOR SUPPRESSIVE AND ONCOGENIC ROLES IN GLIOBLASTOMA: AN INTEGRATED APPROACH WITH DRIVER DBV3

HINA AHSAN

Capital University of Science and Technology (CUST), Faculty of Health and Life Sciences, Department of Bioinformatics and Biosciences, Islamabad, Pakistan.

Email: dbs183002@cust.pk, Orcid ID: <https://orcid.org/0000-0003-4509-4381>

SHAUKAT IQBAL MALIK*

Capital University of Science and Technology (CUST), Faculty of Health and Life Sciences, Department of Bioinformatics and Biosciences, Islamabad, Pakistan.

*Corresponding Author Email drshaukat@cust.edu.pk, Orcid ID: <https://orcid.org/0000-0003-4839-3168>

Abstract

Exome sequencing (exome-seq) by NGS (Next generation sequencing.) has aided in the finding of a significant number of cancer mutations, however challenges persist in translating oncogenomics data into information that is comprehensible and useful for clinical care. We identified the driver genes and the mutation using the database DriverDBV3, which combines exome-seq data, annotation databases, and bioinformatics methods. This database offered Transforming Growth Factor Beta 1 (TGFB1) and driver genes to visualize the correlations between mutations and driver genes in glioblastoma multiform (GBM). The most aggressive brain cancer is the GBM that affects adults with the lowest life expectancy. This study compiles data illustrating the considerable transcriptional and genomic variability of GBM, focusing on 20 clinically relevant driver genes. With a different profile for driver genes and TGFB1 in GBM, a pattern matched the driver genes' involvement in GBM ontogenesis. Also, we discovered TGFB1 overexpression, which was identified as a driver gene in five different aspects based on the mutation score. Also, we discovered a combination of the six-driver genes EGFR, TP53, PTEN, PIK3CA, PIK3R1, and IDH1 with a unique pattern of differential expression and their distinct distribution of somatic mutation, giving them a significant potential to identify the molecular subtype of GBM. Eight computational techniques were used for the GBM dataset to summarize and calculate the results of the driver genes and TGFB1 implicated in GBM. The differential regulation of these genes concerning distinct cellular pathways for GBM patients were also found in our data. This multi-omics analysis will outline future strategies for applying these molecular markers for patient assessment in regular medical practice.

Keywords: Driver genes, Exome sequencing, Glioblastoma, Mutation, Next generation sequencing, TGFB1

1. INTRODUCTION

The cancer genome mutations being identified have significantly risen because of next-generation sequencing (NGS), which also enables the characterization of the histopathological and molecular characteristics of different malignancies. Exome sequencing (exome-seq) has been standard practice in oncogenomics studies over the past few years [1]. Additionally, massive cancer projects like the International Cancer Genome Consortium (ICGC), The Cancer Genome Atlas (TCGA), Therapeutically Applicable Research to Generate Effective Treatments (TARGET), and the Pediatric Cancer Genome Project have generated enormous amounts of data related to cancer

genomics (PCGP) [2]. Although NGS has already assisted researchers in uncovering a sizable number of aberrant events in cancer genomes, it is still challenging to transform this information into scientific information that can be easily acquired and interpreted.

Cancers may be characterized by multiple somatic mutations and are primarily brought by the accumulating effects of genetic changes. However, not all of these mutations contribute to the development of a tumour. Only a small portion of mutations, whereas others, have little impact on cancer development. The driver and passenger mutation has been developed to clarify this concept further.[3]. "Driver" mutations give the tumour cell a selective growth advantage. A "passenger" mutation does not provide a growth benefit but does so in a cell that concurrently or later obtains a "driver" mutation [4].

Although somatically changed genes that change their protein products are present in most solid tumours, the number of non-synonymous mutations varies depending on the kind of cancer. More than 80% of mutations are missense, and the functional effects of these mutations vary greatly depending on their location and function within the protein and the type of amino acid used as a replacement [5]. While many identified missense alterations are neutral passenger mutations, pinpointing cancer driver mutations and are still consider tricky to analyse. Several computational techniques have been developed to anticipate missense mutational effects based on concepts including evolutionary conservation, structural restrictions, and the physicochemical characteristics of amino acids[6]. Machine learning techniques have recently been developed to forecast cancer-causing deleterious mutations[7].

GBM substantially threatens the human population because of its poor prognosis. Individuals with GBM have a meagre chance of survival and often only live for 14 to 15 months after diagnosis [8]. In the current study the mutational data of driver genes and TGFB1 were investigated in the GBM. It was observed that based on IDH1/2 mutational status and the existence of a codeletion of 1p19q, GBMs were divided into three different subtypes: IDH1/2 mut, IDH1/2 mut 1p19q codeletion, and IDH1/2 wt [9]. Several non-synonymous mutations in six genes (EGFR, TP53, PTEN, PIK3CA, PIK3R1, IDH1), were discovered in the glioblastoma catalytic domain and examined using various methods, in silico tools and databases to understand their potential implications on the structure and operation of the GBM driver genes. It is possible that the mutations observed in the GBM events could change the structure and functions of the protein. As a result, we discover the driver genes, TGFB1, and their potential impacts on the protein's structure and function.

In order to discover driver genes, a variety of computational techniques have been used . Algorithms like MUTSIG-CV, OncodriverFM, MuSiC, Simon and DriveDBV3 which are based on the frequency of gene mutations compared to background mutation rates. However, background mutation rates vary significantly among genomic regions and individuals [10]. Using DriverDBV3, we identify driver genes with statistically significant mutation rates in phosphorylation-specific regions. Other methods based on the sub-network approach can identify groups of genes with driver mutations directly from cancer mutation data, with or without prior knowledge of pathways or other information on

protein/genetic relationships[11]. This approach works particularly well when it cannot discriminate between the observed frequencies of passenger and driver mutations, which is when single gene testing fails. Moreover, sub-networks are thought to find cancer-causing genes with minimal recurrence [12]. Most sub-network-based methods, such as Dendrix, Multi-Dendrix, MEMo, MDPFinder, and RME, identify driver genes with the characteristics of mutual exclusion.

In the current study, we introduce the DriverDBV3 database, which integrates exome-seq data, annotation databases (such as 1000 Genome and COSMIC), and several bioinformatics techniques devoted to determining driver genes or mutations in GBM.[13]. DriverDBV3 uses various techniques to determine driver genes and offers many facets of a gene's mutation profile. By analyzing Copy number variation (CNV), methylation patterns, and micro RNA (miRNA) expression profile data, we also conducted an integrated analysis of the TCGA database of GBM Genomic Data Commons database (GDC), intending to complete a new molecular classification and present some new treatment targets for GBM. Recent research has demonstrated that GBM driver genes are essential to numerous biological networks, including the immune system [14]. MiRNAs and CNVs play an essential regulatory role in disease processes and function in typical physiological processes [15]. Although some miRNAs have been associated with the pathophysiology and development of brain tumours, research on long non-coding RNAs (lncRNAs) and miRNAs in brain tumours has lagged [16].

It is essential to comprehend the underlying oncogenic pathways of GBM to develop rational therapeutic strategies. Several driver genes have been linked to GBM in a variety of ways. The protein kinase EGFR is affected by a well-characterized mutation that results in EGFRvIII, a truncated form that is constitutively activated [17]. Furthermore, EGFR overexpression and amplification are significant in GBM. MET amplification, PIK3CA mutations, ERBB2 mutations, CDK4 and CDK6 amplification have all been connected to glioblastoma [18]. Some kinases, like as the kinase WEE1, are discovered to be overexpressed in GBM [19]. It is unclear if other kinases in GBM contribute to mutational activation in the same way.

Hence, it is conceivable to comprehensively analyze the detrimental molecular processes such as genomic instability and somatic mutation of driver genes and TGFB1 in GBM with multi-omics data analysis. We examined the miRNA expression profile data, CNV, and methylation patterns in GBM. This study aimed to classify all dysregulated CNV, MET, and miRNA dysregulation aspects of protein-coding drivers and TGFB1 and also Locus enrichment analysis of these genes linked with patient prognosis.

2 MATERIALS AND METHODS

2.1 Data collection

The TCGA database had 163 tumour samples and 207 standard samples in the glioblastoma dataset. We only used samples for which data for the four genomic platforms of RNA expression, gene mutation, CNV, and gene fusion were available in the DriverDBV3 database. The most recent RNA sequencing and exome sequencing data

from TCGA were obtained from the GDC data portal, for which the pre-processing data method is described in the DriverDBV3 portal[20]. This portal includes the TCGA 2BED tool, for Methylation data from a firehose, for the TCGA R package, "TCGA bio links," and CGC, which was collected from COSMIC and the NCG6.0 database, was used to define cancer-related genes. These pairs' mutation and CNV data were obtained through the data portal. Using the Pathway Mapper database, the representative genes of eleven traditional pan-cancer signalling pathways were obtained[21]. In the DriverDBV3 online database, at least seven algorithms (or 50 percent of all algorithms) predicted the driver genes that were the subject of this investigation [22].

2.2 Prognostic analysis of glioblastoma

TCGA glioblastoma sample mutational characteristics were categorized using gene expression profiles. PAM50 algorithm with the Integration of DriverDBV3 was used[23]. Using Kaplan-Meier analysis, the predictive analysis was carried out on the samples.

2.3 Screening and identification of Driver Genes

DriverDBV3 used eight computational techniques to locate cancer driver genes. All mutations are used to identify driver genes by four approaches based on mutation frequencies: MutSigCV, OncodriverFM, Simon, and ActiveDriver. The sub-network-based approaches were implemented using MEMo, Dendrix, MDPFinder, and NetBox. The DriverDBV3 database having well-known driver gene prediction methods were then utilized to determine the 80 driver genes. We defined driver genes as genes that were recognized as driver genes by more than seven algorithms [24].

2.4 DNA-Level differences and Mutation annotation

Our study evaluated the GBM driver gene TGFB1 and ten common oncogenic pathway genes for DNA-level alterations like gene mutation, gene fusion and CNV. A thorough investigation of the prevalence of DNA changes and the number of samples with DNA changes was conducted for each subtype. All mutations were mapped to well-known databases, and various bioinformatics tools are displayed in the Annotation module. DriverDBV3 uses data gathered from numerous databases, including NHLBI GO ESP, dbSNP, COSMIC, 1000 genomes, ClinVar (<http://www.ncbi.nlm.nih.gov/clinvar/>), GWAS catalogue, HGMD-PUBLIC, and OMIM (<http://omim.org/>), to annotate known variations[25]. To forecast the effects of each mutation, including non-synonymous coding, stop gained/lost, and frameshift, we employed SnpEff and VEP. Also, we assigned a Driver Score of 7 to each mutation based on the 7 algorithms that classify the mutation as harmful [26].

2.5 Functional Analysis

In order to evaluate the interactions between driver genes discovered in a collection of cancer samples using one or more methods, we defined three levels of biological interpretation of Gene Ontology, Pathways enrichment, and Protein/Genetic Interaction between the driver genes. The Gene Ontology task was carried out by computing the GO graph's topology and visualizing the connections between GO keywords and genes using

Bioconductor programmes. The datasets were employed from KEGG, REACTOME, and MSigDB to annotate driver genes in the "Pathway" analysis. The Protein/Genetic Interaction was deciphered using the three databases BioGRID, iRefIndex and IntAct. Traditional Fisher's exact test and $-\log(P \text{ value})$ was used to assess each GO word and Pathway category in the Gene Oncology and Pathway studies. The Cytoscape Web tool was included in the DriverDBV3 web interface's "Pathway" and "Protein/Genetic Interaction" sections enabling interactive network visualization [11].

2.6 Ethical Approval and Resource Sharing

This retrospective study received approval by the ethical review board of the Capital University of Science and Technology (CUST), Islamabad, Pakistan. All the patients provided consent to the scientific use of their data. The biopsy samples of thirty-three (23 males, 10 females, median age 50 ± 13 years) patients of high grade gliomas were collected from various surgery departments, public sector tertiary care hospitals of Pakistan who underwent brain surgery between January 2018 and December 2021. Before sample collection, none of the participants in the study had radio therapeutic or chemotherapeutic treatment.

2.7 Quantitative RT-qPCR Analysis

After ablation, 33 tissue biopsy samples were liquid nitrogen-snapped and stored at -80°C until RNA extraction. To extract total RNA, the TriZol reagent was utilized. Using the SYBR® Green Master Mix kit, qPCR was carried out to amplify the specific PCR products of the three genes proposed in this investigation using Superscript II reverse transcriptase (Invitrogen, Paisley, UK) (Thermoscientific, CA, USA). The $2^{-\Delta\Delta\text{Ct}}$ technique and β -actin as the reference gene was used to analyze the mRNA expression of each gene.

2.8 ELISA

Before protein extraction, high-grade glioma biopsy samples were frozen in sterile containers and kept at -80°C . Protein-specific ELISA kits (Abcam Elisa kits USA) were used to quantify the levels of the gene TGFB1 following the manufacturer's instructions. Right away, the specific binding optical density at 450 nm was determined by a spectrophotometer.

3. RESULTS

3.1. Identification of driver genes in glioblastoma network and functional analysis

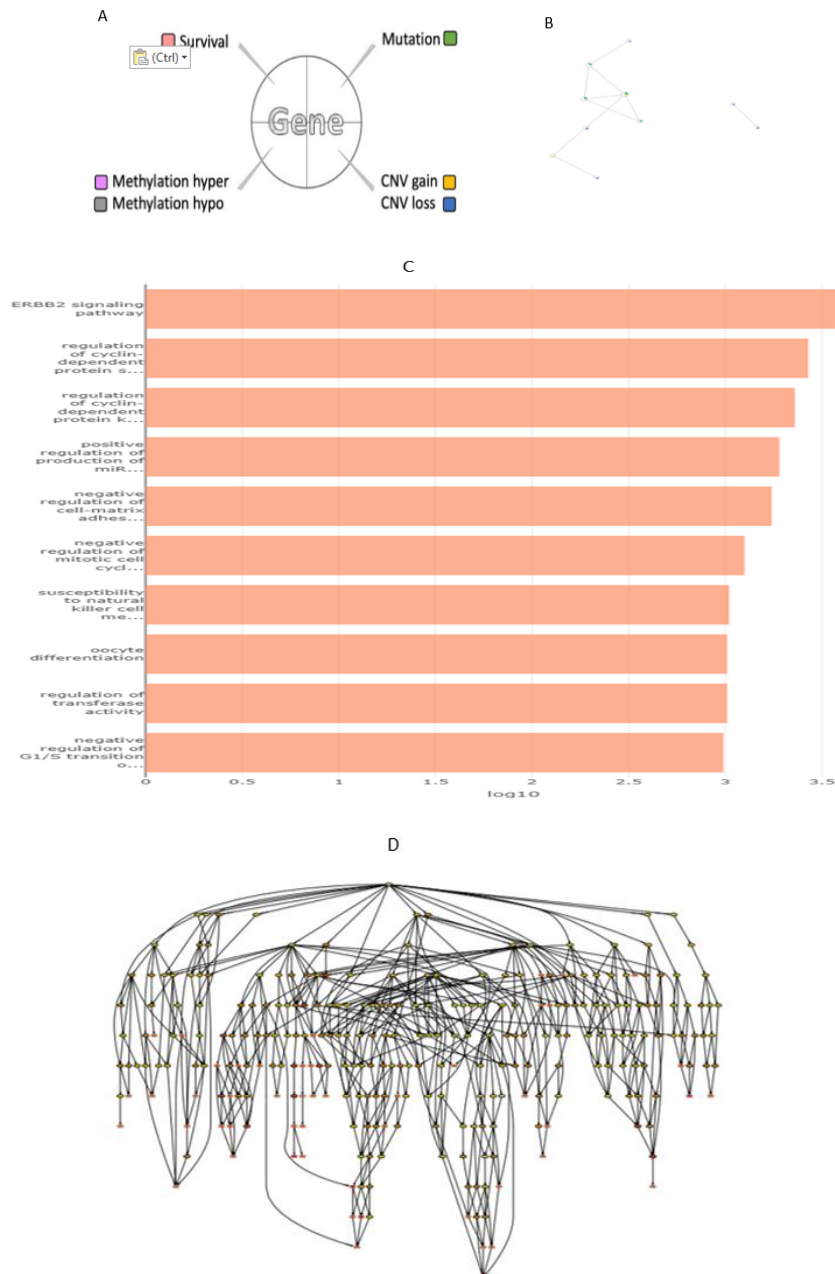
The GBM summary network (Fig. 1A) showed the relationship between driver genes and miRNA drivers in glioblastoma. Driver genes have a variety of characteristics, and colour-coded nodes identify them; yellow nodes identify MicroRNA (miRNA) drivers. These nodes are joined by lines to depict the protein-protein interactions (PPIs) in the STRING database and synergistic effects, which are defined as situations in which the hazard ratio (HR) of two genes is larger than 1.5 times that of each gene. Moreover, miRTar Base keeps track of how miRNAs and genes interact (Fig.1B). We predicted the driver genes of glioblastoma samples in the TCGA database using the DriverDBV3 online database,

as shown in table 1, in order to better understand the molecular characteristics of glioblastoma. Our top 20 driver genes are Epidermal Growth Factor Receptor (EGFR), Phosphatidylinositol-4,5-Bisphosphate 3-Kinase Catalytic Subunit Alpha (PIK3CA), Isocitrate Dehydrogenase (NADP(+)) 1 (IDH1), Tumor Protein P53 (TP53), Phosphatase and tensin homolog (PTEN), Rh Blood Group D (RHD), Phosphoinositide-3-Kinase Regulatory Subunit 1(PIK3R1), leucine rich repeat containing 37A (LRRC37A), Glutathione S-Transferase M1(GSTM1), Signal Regulatory Protein Beta 1(SIRPB1), Sodium/potassium/calcium exchanger 3(SLC24A3), Major Histocompatibility Complex, Class II, DR Beta 5 (HLA-DRB5), osteosarcoma amplified 9(OS9), Carboxy-terminal domain RNA polymerase II polypeptide A small phosphatase 2 (CTDSP2), Maternal Embryonic Leucine Zipper Kinase (MELK), Zinc Finger And BTB Domain Containing 42 (ZBTB42), UDP Glucuronosyltransferase Family 2 Member B17 (UGT2B17), Energy Homeostasis Associated (ENHO), Cyclin Dependent Kinase Inhibitor 2B (CDKN2B) and contact in associated protein family member 3B (CNTNAP3B). We employed DriverDBV3 having more than seven algorithms to predict driver genes simultaneously to improve the accuracy of our results. Through network analysis, 80 driver genes were expressed, and the top 20 driver genes of glioblastoma were screened for gene ontology based upon significant log values of biological process ERBB2 signaling pathway, regulation of cyclin-dependent proteins, regulation of cyclin-dependent proteins kinases, positive regulation of production of miR and negative regulation of mitotic cell cycle (Fig.1C-D). The twelve gene set collections from seven public database KEGG, PID, Biocarta, Recatome, MsigDB, miRTar, and miRWalk are used in the pathway analysis. The significant genes at KEGG were PIK3CA, PIK3R1, TP53, EGFR, PTEN, CDKN2A and CNTNAP3B at $-\log_{10}$ (p-value) (Fig.1E). Similarly cellular functional analysis showed phosphatidylinositol 3-kinase complex, cytoplasmic part, region of cytosol, cytoplasm and apical plasma membrane shown highest log values (Fig.1F). Lastly the molecular functions of driver genes of GBM also shown significant log 10 values in respect to natural killer cell lectin-like receptor, insulin substrate insulin binding and cyclin dependent protein serine threonine in (Fig.1G).

Table 1: Top 20 driver genes of glioblastoma summary table

cancer	gene	CGC	NCG6.0	mutation	CNV	methylation	miRNA
GBM	EGFR	1	1	12	1	0	
GBM	IDH1	1	1	7	0	0	
GBM	PIK3CA	1	1	9	0	0	
GBM	PIK3R1	1	1	9	0	0	
GBM	PTEN	1	1	11	0	0	
GBM	TP53	1	1	12	0	0	
GBM	RHD	0	0	0	-1	0	
GBM	LRRC37A	0	0	0	1	0	
GBM	GSTM1	0	0	0	-1	0	
GBM	SIRPB1	0	1	0	1	0	
GBM	SLC24A3	0	0	0	1	0	
GBM	HLA-DRB5	0	0	0	1	0	
GBM	CTDSP2	0	0	0	1	0	
GBM	OS9	0	0	0	1	0	

GBM	MELK	0	0	0	-1	0	
GBM	ZBTB42	0	0	0	-1	0	
GBM	UGT2B17	0	0	0	-1	0	
GBM	ENHO	0	0	0	-1	0	
GBM	CDKN2B	0	1	0	-1	0	
GBM	CNTNAP3B	0	0	0	-1	0	



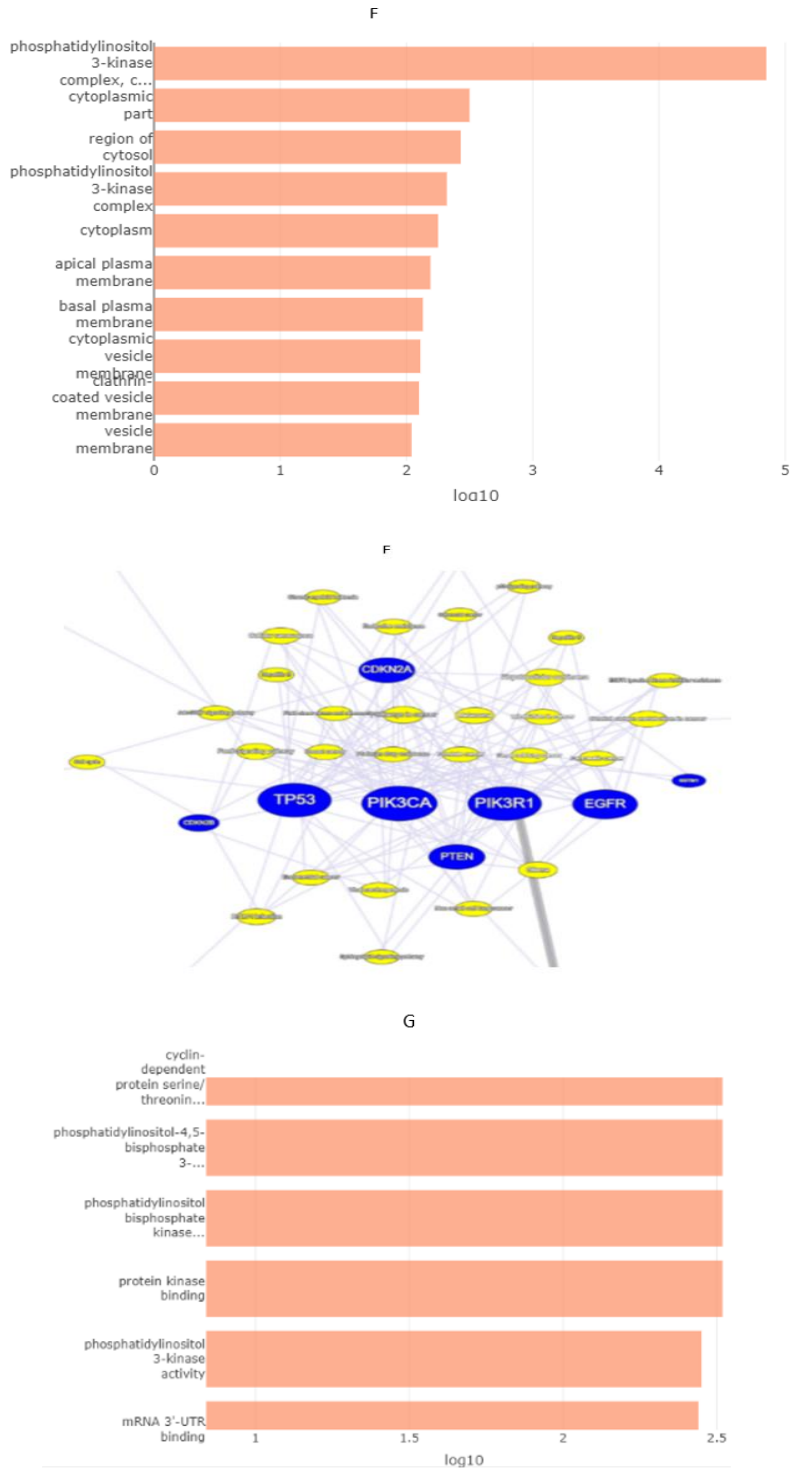
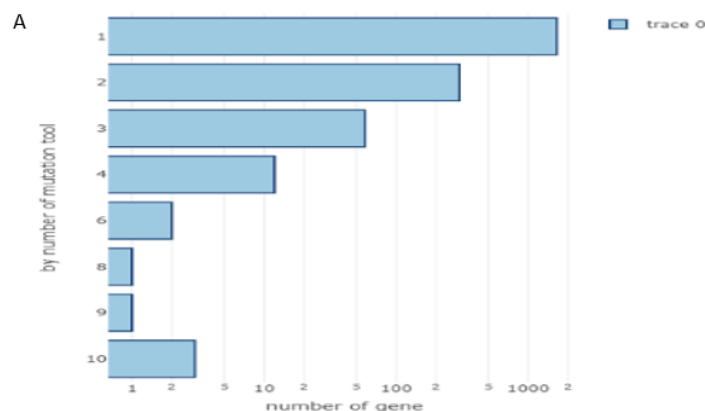


Fig 1: Analysis of the driver genes in glioblastoma. A) The glioblastoma network presents the relationships between driver genes and miRNA drivers in a specific cancer type. B) In the Summary panel, a network shows the drivers for mutation,

CNV, methylation, and miRNA, each represented by a different colour grid in the node. Protein-protein interactions between nodes make up the string database's interactions. Determining which two genes' hazard ratios (HR) are larger than 1.5 for each gene. C-D-F-G) with a statistically significant value of $\text{Log}_{10} P = 0.05$, the functional annotation section provides gene ontology of functional analysis of driver genes in biological, cellular, and molecular processes. E) The Pathway section contains 12 gene set collections collected from 7 open-access databases: at $-\log_{10}$ for KEGG (p-value)

3.2. The mutational and survival analysis of driver genes

The current insilico studies have shown that glioblastoma has many driver gene mutations. To more clearly establish the impact of driver genes on the prognosis of glioblastoma patients, we analyzed the driver gene mutations in the erroneous modifications of commonly altered genes and essential cancer genes in many signalling pathways. The bar graph depicted the top 30 major mutation drivers as determined by multiple computational tools, including the new tools CoMET, Mutex, and DriverML. (Fig. 2A). It was observed that the change frequency of driver genes EGFR, TP53, PTEN, PIK3CA, PIK3R1, IDH1 were more significant, and we discovered these driver genes had a higher proportion of mutations. This graphic shows the relationships between the top 30 mutation driver genes and cancer patients with the integration of tools as shown in figure 2B-2C. The impact of driver gene mutations on the prognosis of GBM patients was then examined. Based on whether the driver gene had a mutation, CNV, or gene fusion, we separated the samples of each subtype into an altered group and a non-altered group. Our investigation discovered that CRISP2, DCSTAMP, and MLPH had a poor survival effect and a substantial hazard ratio. The orange and green nodes indicate the survival genes with $\text{HR} > 1$. For each synergistic survival event, Kaplan-Meier plots were generated using the comparison of all high against others and four expression-based groups (all high, low/high, high/low, and all low). The hazard ratio values for CRISP2, DCSTAMP, and MLPH were 2.75, 2.55, and 2.81, respectively, as shown in figure 2D.



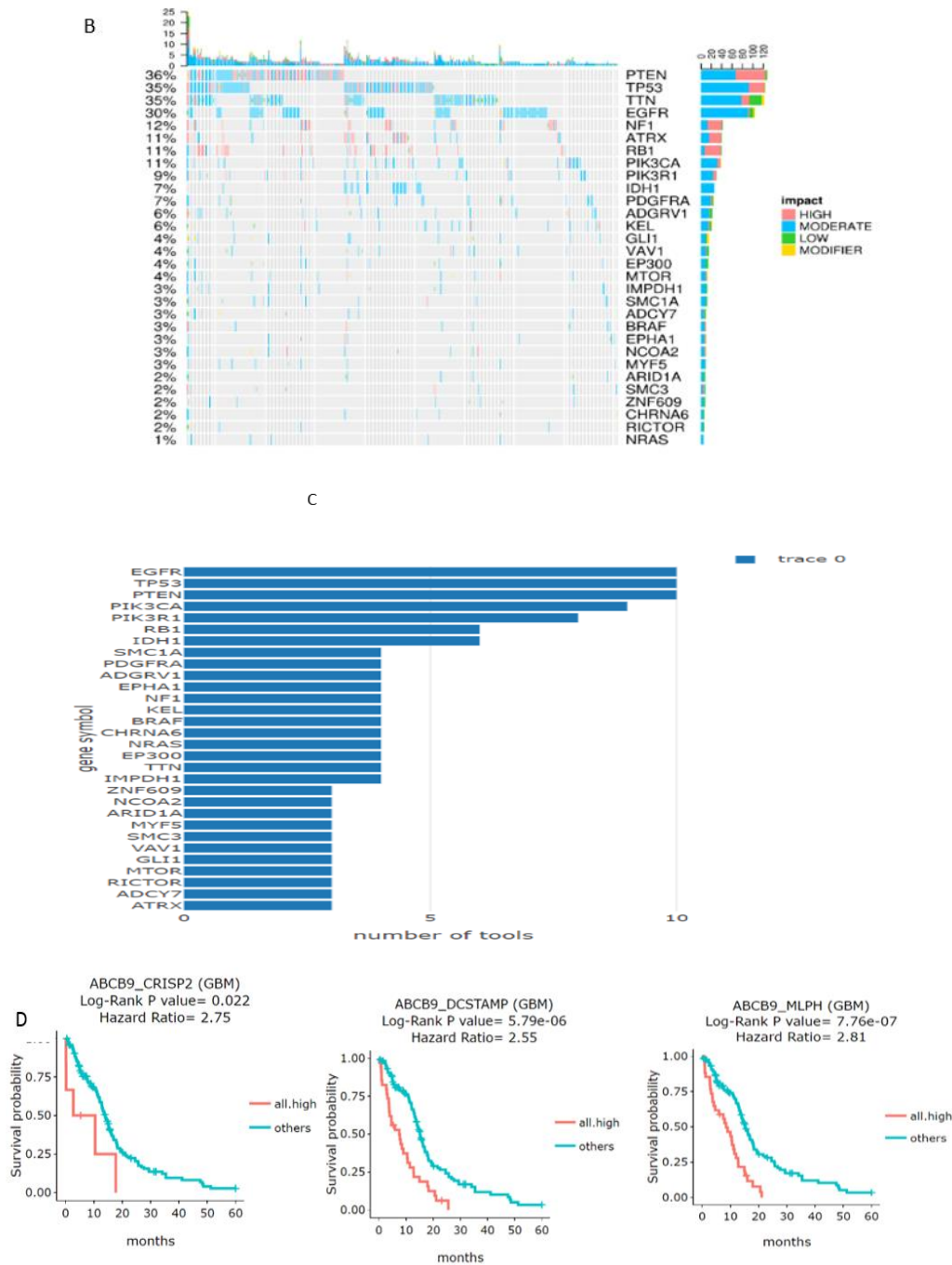


Fig 2 | Mutational and survival Analysis of the driver genes in glioblastoma. A) The plot indicates defined mutation driver numbers by a different number of computational tools according to the mutation summary table. **B)** Using cancer patient samples on the x-axis and the top 30 genes on the y-axis, this graphic shows the relationships between the top 30 mutation driver genes and cancer patients. **C)** This plot shows the top 30 genes on the y-axis and the number of

tools by which they are defined on x-axis. D) This section includes all gene pairs with HR fold change greater than 1.5 in both directions. The patients are divided into groups depending on the patients' levels of gene expression for each gene pair. The hazard ratios for CRISP2, DCSTAMP, and MLPH were 2.75, 2.55, and 2.81 respectively. The survival probabilities of the patient groups are then contrasted throughout the months, as demonstrated in the plots with a significant p-value of 0.05

3.3. CNV, MET and miRNA-define dysregulation features of protein-coding drivers and Locus enrichment analysis of Glioblastoma

In order to analyse the aberrant shifts and changes in gene expression and to define CNV and methylation dysregulation events, iGC, DIGGIT, and methylmix were used to identify CNV dysregulation events. Whereas the ELMER and methylation mix were used to identify methylation dysregulation incidents to analyze the aberrant shifts and changes in gene expression and define CNV and methylation dysregulation events by driverDBV3. As a result, this aligns CNV and methylation computational algorithms and interpretations of abnormal miRNA regulation with negative correlation coefficients between miRNA and driver genes. Using a heat map, we identify the top 30 drivers, CNV and methylation panels which also showed these novel traits in a similar way (Fig. 3A). Similarly percentage bar charts showed significant gain in percentage of genes are EGFR (81%), LANCL2 (79%), SEC61G (78%), VOPP1 (77%), NIPSNAP2 (73%), MRPS17 (73%), ZNF713 (73%), PSPH (73%), SUMF2 (72%) and the genes with the significant loss functions were CDKN2A (71%), CDKN2B (70%), MTAP (67%), KLHL9 (60%), MLLT3 (54%) and TUSC1(50%) as shown in (Fig. 3B). The most significant regions with identified CNV events were 1,3,4,6,7,9,12,13,14,15,17,20,22 and Y, as indicated in locus enrichment, which were also carried out to comprehend those regions that include CNV/differentially methylated events (Fig. 3C).

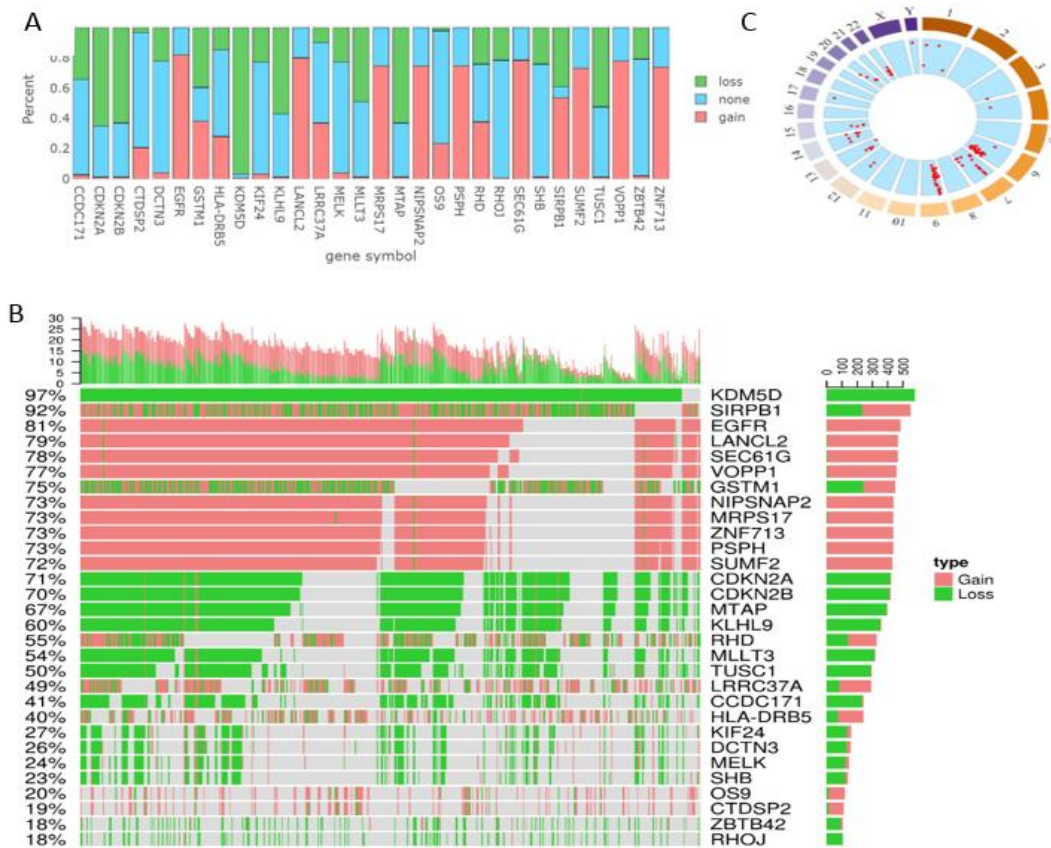
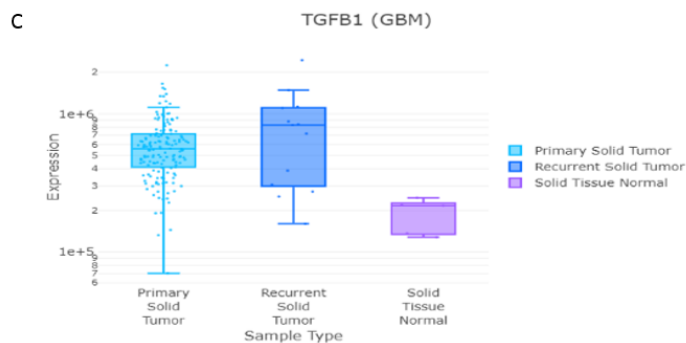
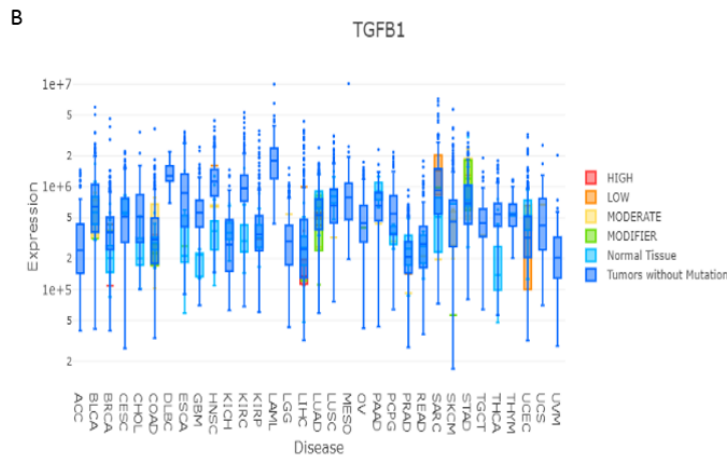
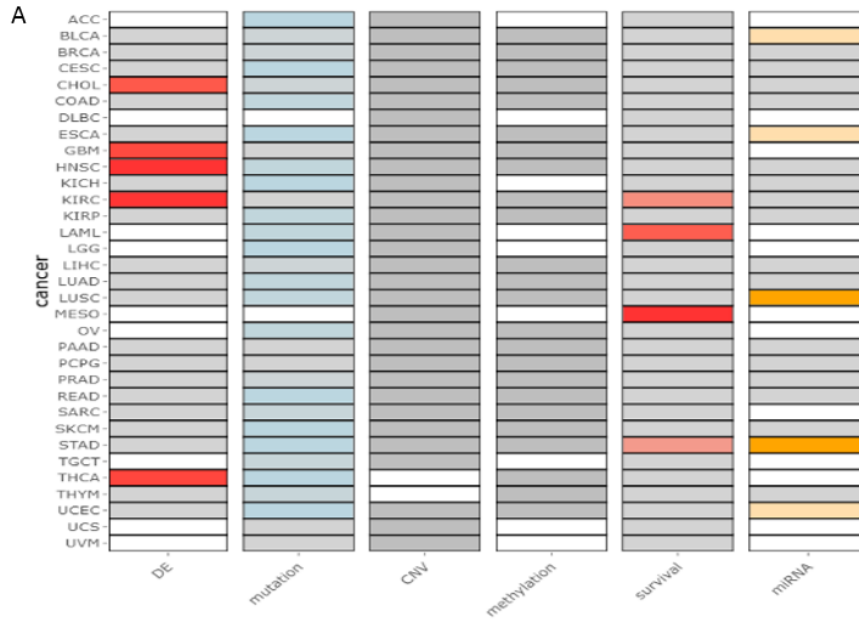


Fig 3 | CNV, MET and miRNA-define dysregulation features in GBM. A) The top 30 CNV drivers are shown on a Heat Map in the CNV panel. B) A percentage bar chart in the CNV panel displays the sample proportions for the top 30 CNV drivers. C) Based on the locus enrichment analysis's findings, a circle graph in the CNV panel highlights the driver's loci on each chromosome with a red dot

3.4. Differential expression of TGFB1 in pan-cancer and GBM biopsy samples due to mutations

Differential expression of the TGFB1 gene concerning various cancer types is visualized using the Gene Summary analysis (Fig. 4A). The Differential Expression (DE) indicated Red block in GBM. The boxplots show the expression patterns across all cancer types for TGFB1. The expression is grouped by mutation class, showing the expression of TGFB1 in GBM in between $1e+5$ to $1e+6$ (Fig. 4B). The distribution of expression inside each GBM tumor type is shown in detail by the plot in a similar way. TGFB1 expression shown in Normal Solid Tissue was $2.1655e+5$, Primary Solid Tumor was $P=5.5846e+5$ and expression of TGFB1 shown in Recurrent Solid Tumor was $8.2995e+5$ (Fig. 4C). To evaluate the mutational status of TGFB1 in GBM, we quantified the expression of TGFB1, and it was observed that protein expression was significantly increased in high grade glioma biopsy samples. We also examined the gene expression of targeted gene among grade III and gradeIV (GBM) specimen sections within the tumour and tumor-associated

normal tissue (TANT). All tissue samples were initially cut from four specimen regions, but samples with sufficient RNA quality and quantity were subjected to RT-PCR gene expression analysis (Fig. 4D). These data are consistent with ELISA findings (Fig. 4E).



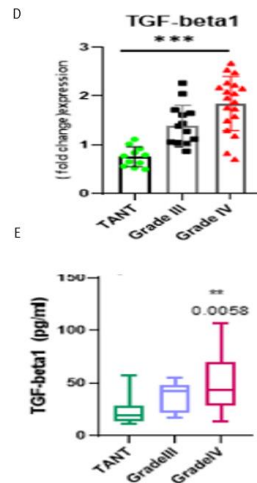


Fig. 4 | Differential expression of TGFB1 in pan-cancer and in GBM biopsy samples due to mutations. A) Multi-omics characteristics in the major cancer types are shown in a summary graph for TGFB1. B) A percentage bar chart in the CNV panel represents the top 30 CNV drivers sample proportions. C) TGFB1 expression shown in Solid Tissue Normal was 2.1655×10^5 , Primary Solid Tumor was $P=5.5846 \times 10^5$ and expression of TGFB1 shown in Recurrent Solid Tumor was 8.2995×10^5 . D) Expression levels of TGFB1 in biopsy tissue of GBM through RT-PCR. The graphs were plotted with the Graph Pad Prism 9 software. E) Enzyme-Linked Immunosorbent Assay validated the expression of DEGs in GBM patients

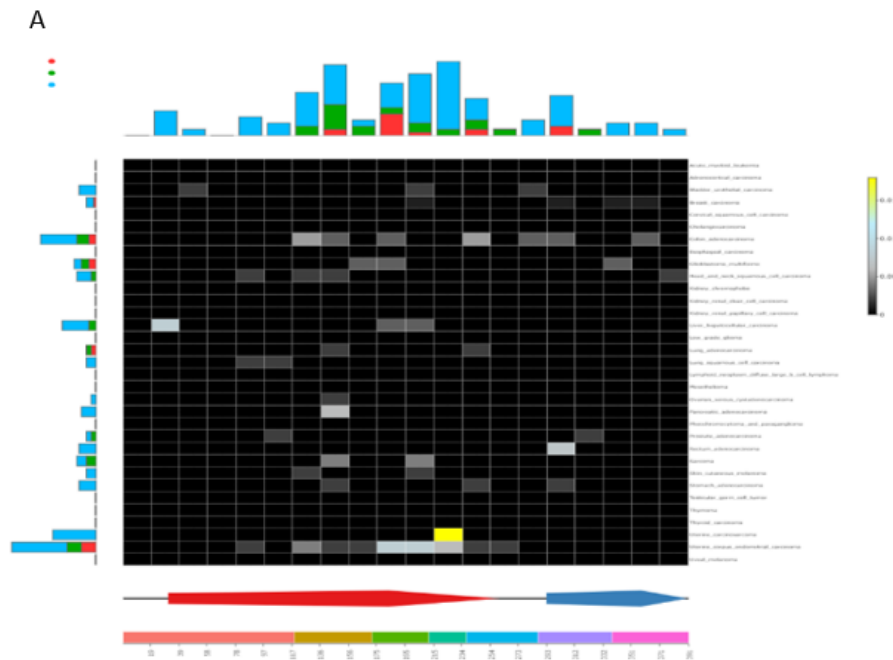
3.5. CNV, MET and miRNA-define dysregulation features of TGFB1 of GBM

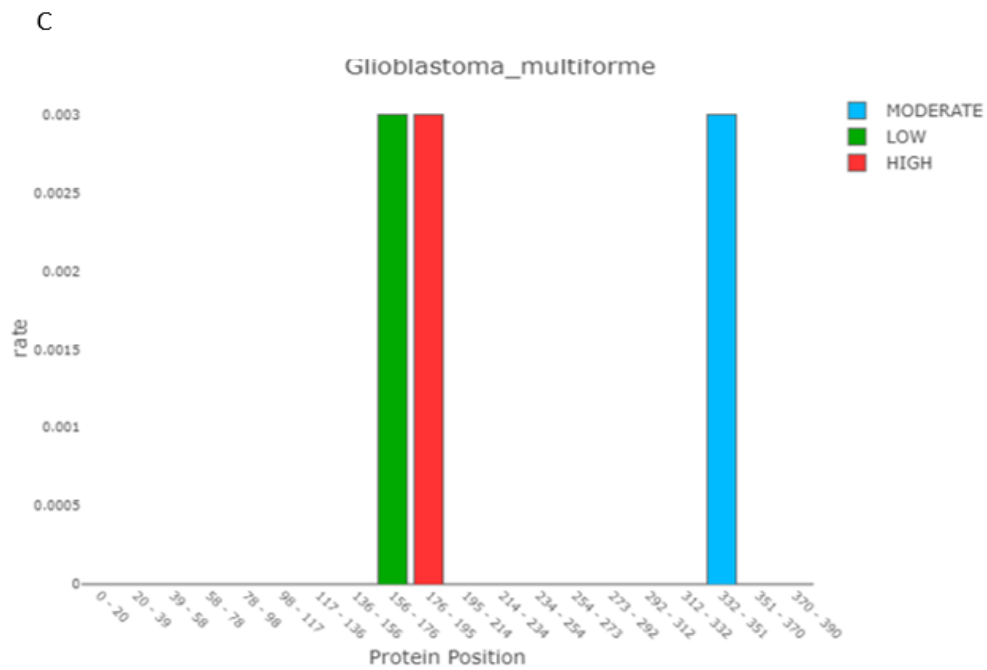
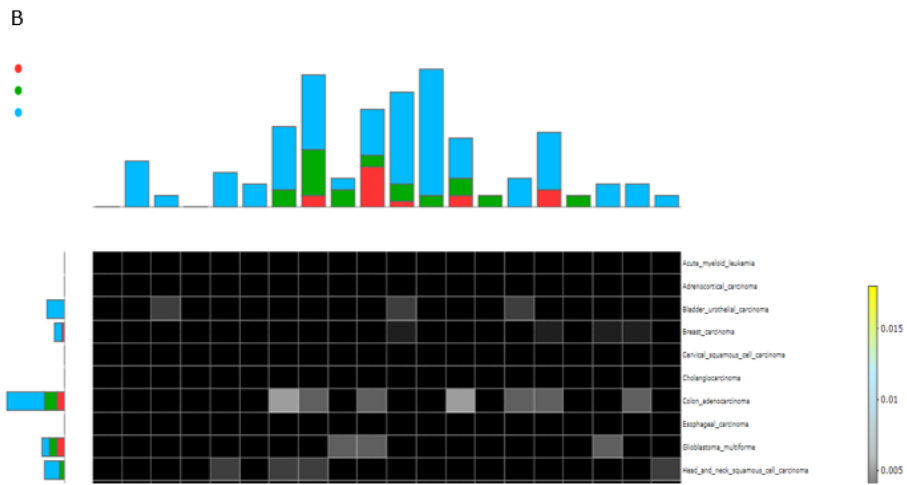
The gene mutation function provides visualizations to illustrate mutation statistics corresponding to protein regions and exons in multiple cancer types. This heat map displays the frequency of TGFB1 mutations at various protein locations in various cancer types (Fig. 5A). The mutation rate is calculated as the sample count divided by the mutation count and is shown by a colour scale. (Mutation rate = mutation count/sample count). The heat map shows mutations in 3 samples, the mutation rate =0.003 at protein-region 156- 176, for 2nd sample the mutation rate =0.003 at protein- region 176- 195 and 3rd sample, the mutation rate =0.003 at protein- region 332- 351(Fig. 5B). The bar chart also showed the mutation rate of the TGFB1 and its protein positions for GBM. The green colour bar showed a low mutation rate at protein- region 156- 176, the red color bar showed high mutation rate at protein- region 176- 195 while blue color bar showed moderate mutation rate at protein- region 332- 351 (Fig. 5C). The Gene CNV function uses bioinformatics algorithms to visualize the copy number gain or loss of a user-selected gene across various cancer types. The scatter plot displays the relationship between CNV value and gene expression (y-axis) (x-axis). The expression levels are shown in the left boxplot, and the CNV values for each type of CNV are shown in the bottom boxplot. The TGFB1 showed 638.2k median expression copy number gain while the segment mean ranges from 0.489 at 0 to 0.5. Similarly, the TGFB1 showed 320.7k median expression copy number loss while the segment mean ranges from median -0.66

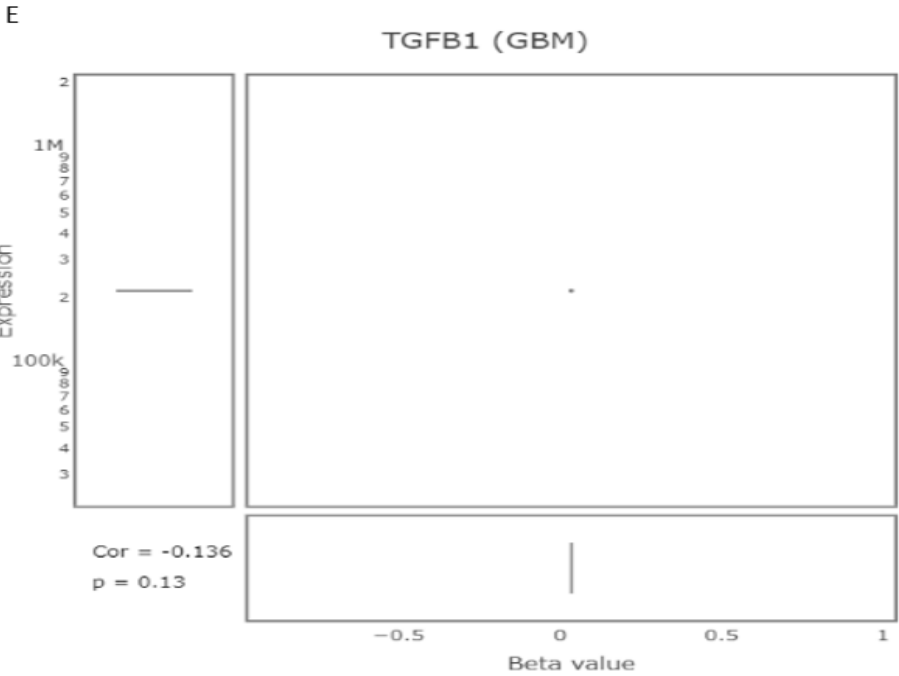
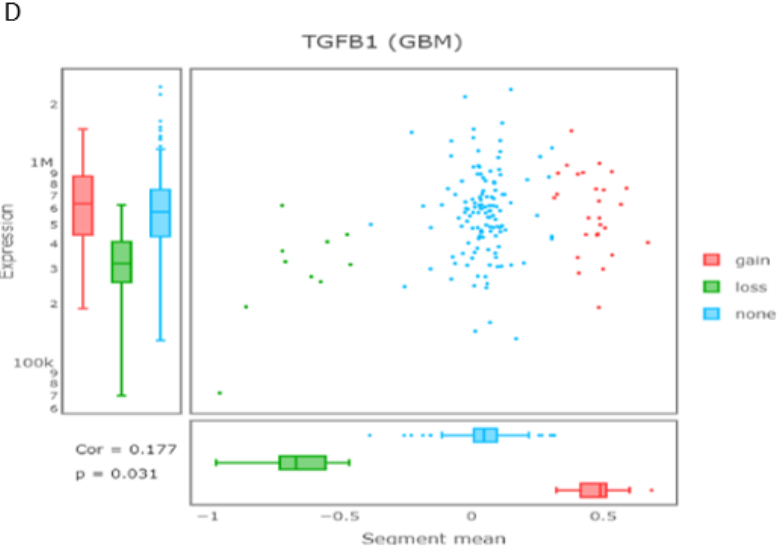
at -1 to -0.5. While TheTGFB1 showed 580.4k expression copy number none while the segment mean ranges from 0.0480 (Fig. 5D). The relationship between gene expression and beta value is similarly shown in the "Methylation" section. In order to demonstrate a detailed view of the methylation distribution and correlation in GBM, this graph combines a scatter plot and boxplot. The value of TGFB1 in the GBM data set considers as usual, having the value 0.0353K, Cor =-0.136 while p=0.13 as shown in (Fig. 5E). The gene miRNA network depicts the relationships between a TGFB1 and miRNAs. Table 2 lists details for seven miRNA genes. Twelve prediction tools or experimental validations that miRTarBase recorded contributed to defining the interactions. Predicted relations are shown as dotted lines, while validated relations are shown as solid lines. A minimum of six, eight, or ten tools can further filter the predicted relations by driverDBV3 (Fig. 5F).

Table 2: Gene-miRNA of glioblastoma table

cancer_type_abbr	Mirbase_mat_id	Gene symbol	ensg	validated	number_of_tool	pearson_cor	pearson_pv	spearman_cor	spearman_pv	kendall_cor	kendall_pv
BLCA	hsa-miR-93-5p	TGFB1	ENSG00000105329	1	0	-0.243	7.07E-07	-0.32	5.13E-11	-0.215	1.03E-10
ESCA	hsa-miR-93-5p	TGFB1	ENSG00000105329	1	0	-0.24	2.20E-03	-0.314	5.40E-05	-0.207	1.01E-04
LUSC	hsa-miR-17-5p	TGFB1	ENSG00000105329	1	0	-0.274	1.22E-09	-0.368	1.05E-16	-0.254	1.49E-16
LUSC	hsa-miR-93-5p	TGFB1	ENSG00000105329	1	0	-0.298	3.24E-11	-0.334	9.75E-14	-0.228	1.07E-13
STAD	hsa-miR-17-5p	TGFB1	ENSG00000105329	1	0	-0.271	1.11E-07	-0.388	7.76E-15	-0.26	7.46E-14
STAD	hsa-miR-93-5p	TGFB1	ENSG00000105329	1	0	-0.35	3.83E-12	-0.457	0.00E+00	-0.31	4.88E-19
UCEC	hsa-miR-93-5p	TGFB1	ENSG00000105329	1	0	-0.205	1.73E-06	-0.328	7.59E-15	-0.224	1.01E-14







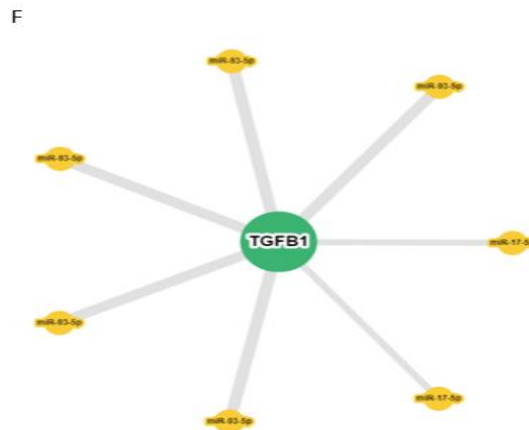


Fig 5 |CNV, MET and miRNA-define dysregulation features of TGFB1 of GBM. A) The heat map indicates the mutation rate of TGFB1 at different protein positions in several cancer types. B) The heat map shows mutations in 3 samples. The mutation rate =0.003 at protein- region 156- 176. For the 2nd sample, the mutation rate =0.003 at protein- region 176- 195; for the 3rd sample, the mutation rate =0.003 at protein- region 332- 351. C) The bar chart also showed the mutation rate of the TGFB1 and its protein positions for GBM. The green colour bar showed a low mutation rate at protein- region 156- 176, and the red colour bar showed a high mutation rate at protein- region 176- 195, while the blue colour bar showed a moderate mutation rate at protein- region 332- 351.D) This graph combines a scatter plot and boxplot to demonstrate a thorough picture of the CNV distribution and correlation in GBM. E) The gene methylation function provides Visualizations of the methylation pattern of TGFB1 across GBM. F) The gene miRNA function provides visualizations illustrating the relations between TGFB1 and miRNAs across GBM.

DISCUSSION

DriverDBV3 imparts the extensive exome-seq data set published recently by combining driver gene analysis from various approaches and visualising mutation data according to many factors. Based on various presumptions and characteristics, various bioinformatics techniques have been employed to discover driver genes, each offering a different perspective. Gene ontology, pathway and protein/genetics interaction are the three levels of biological interpretation offered by driverDBV3, which integrates the study results of one or multiple methods [27]. The results of this visualization will help analyze the links between the driver genes. This study illustrates a driver genes found in glioblastoma multiforme (GBM). The 20 driver genes discovered were TP53, EGFR, IDH1, PIK3CA, PIK3R1, PTEN, LRRC37A, GSTM1, SIRPB1, SLC24A3, OS9, MELK, ZBTB42, UGT2B17, ENHO, and CDKN2B (each gene by at least 7 methods by driverDBV3). The important six genes listed (EGFR, TP53, PTEN, PIK3CA, PIK3R1, IDH1) are recognized as crucial in developing GBM tumors due to harmful mutations [28]. Therefore, through integrated analysis 12 mutations reported in the EGFR gene, 12 in the TP53 gene, 11 in

the PTEN gene, 9 in the PIK3CA gene, 9 in the PIK3R1 gene, and 7 in the IDH1 gene. Our functional analysis reveals that 20 genes are involved in cell cycle-related categories, including phosphatidylinositol 3-kinase complex, cytoplasmic part, region of cytosol, cytoplasm, and apical plasma membrane, as well as in the molecular functions of driver genes of glioblastoma in relation to natural killer cell lectin-like receptor, insulin substrate insulin binding, and cyclin-dependent protein serine-threonine. A few abnormalities that cause primary glioblastoma (GBM) to proliferate and invade angiogenetically are EGFR overexpression, PTEN (MMAC I) mutation, CDKN2A (p16) deletion, and, less commonly, MDM2 amplification [29]. In secondary GBM, TP53 mutations are typically the first genetic changes found [30, 31]. Moreover, the IDH mutation was linked to the G-CIMP (Glioma CpG Island Methylation Phenotype) of enhanced DNA methylation[32]. Somatic mutations in the iSH2 domain of PIK3R1, which encodes P85, provide a different way for tumours to downregulate the PI3K signalling cascade. This mutation also promotes the development of GBM [33]. In engineered mouse models and primary human cell systems, activation of PI3K signalling through PTEN loss or AKT overexpression has also been shown to promote the development of GBM tumours [34], validating the clinical significance of changes in this pathway that have been discovered in GBM patients [35]. Similarly, EGFR gene amplification and mutations play a significant genetic role in GBM, increasing the expression of both the wild-type (EGFR_w) and mutant oncogenic versions of the EGFR [36]. It has been shown that the mutant receptor may activate PI3K without PTEN loss because EGFR_v strongly correlates with the activation of mTOR in vivo[37]. At least 60% of GBM have been found to have deregulated phosphatidylinositol 3-kinase (PI3K) signalling pathways due to genetic changes in the PTEN tumour suppressor gene on 10q23 at the level of LOH, mutation, and methylation[38]. Poor survival in anaplastic astrocytoma and GBM is correlated with loss of PTEN function by mutation or LOH, indicating that PTEN is involved in patient outcome [39]. TP53 mutations have been discovered to directly reduce overall survival in glioma patients [40]. The DNA-binding domain has missense mutations, accounting for 75% of p53 mutations[41]. The components of this pathway (PTEN, p110, p85, and probably receptor tyrosine kinases like EGFR) are the starting locations for signalling accelerated invasion among the prevalent alterations that promote GBM development and progression. Given that 46% of GBM patients have mutually exclusive mutations in PIK3CA, PIK3R1, and PTEN, the PI3K pathway is a promising therapeutic target [42].

Poor survival effects were identified for the other three genes, CRISP2, DCSTAMP, and MLPH. Many physiological and pathological processes, such as immunology, venom toxicity, reproduction, and cancer biology, have been linked to the CAP family of proteins [43]. Cell-cell adhesion, a crucial step in establishing and maintaining tissue patterns during development and a crucial mechanism during invasion and metastasis, one of the hallmarks of cancer, is mediated by DCSTAMP and MLPH [44] [45].

TGF- β is widely known as a cytokine that promotes invasion, angiogenesis, and the inhibition of the immune system, making it a known driver of GBM invasion [46]. Hence, in addition to its varied roles in the formation of GBM, TGF- β adds a new function as a result of our findings. Due to its effects on cell proliferation, tumour invasion,

angiogenesis, immunosuppression, and the preservation of the steamininess of glioma stem cells (GSCs), the TGFB1 pathway has been recognized as a mediator in the initiation and progression of gliomas[47]. We quantified the Expression of TGFB1 to evaluate the mutational status of the protein in GBM. It was found that the protein expression was markedly elevated in GBM biopsy samples. Human investigations have shown that malignant glioma tissues overexpress TGFB1 while normal brain tissues are undetectable, further indicating that TGFB1 plays a role in the development of gliomas [48].

TGFB1 driver gene mutation data were visualized using driverDBV3 through Insilico analysis. Hotspot mutation sites (in the protein's centre and end), particularly in the "Mutation Percentage of TGFB1" were identified and computed. It was noted in earlier studies, missense and deep deletion mutations of TGFBI were the most prevalent in GBM[49]. This has been identified as the cause of the suboptimal response to TGFB1 inhibitors in GBM with mutations in the extracellular domain. Further to EGFR mutations at the kinase domain (KD), mutations at the extracellular domain activate EGFR in GBM. This has been observed as the cause of the poor response of GBM to EGFR inhibitors (such as erlotinib) that target the active kinase conformation in GBM with mutations in the extracellular domain [50]. Our calculations successfully simulated this pattern, also visible in the 'Mutation Profile' of TGFB1 in DriverDBV3. Study showed that miRNA expression is aberrant in cancer due to miRNA gene amplification, loss, translocation, epigenetic silencing, dysregulation of transcription factors (such as p53 and c-Myc), and flaws in the enzymatic machinery involved in synthesis[51].

The TGFB1 exhibited a 638.2k median expression copy number gain, while the segment means 0.489 at 0 to 0.5. Similarly, the bar chart's colours represent a functional impact of mutation. Similar to the theTGFB1, the segment means for the TGFB1 ranges from median -0.66 at -1 to -0.5 and 320.7k median expression copy number loss. When DriverDBV3 determined the segment mean from 0.0480, TheTGFB1 displayed 580.4k expression copy number none.

Finding mutations that cause cancer still poses a considerable difficulty, according to several studies that evaluated the effectiveness of current techniques for predicting harmful mutations. So, to explain the harmful intensity of a mutation and to emphasize the hotspot mutation zone, we employed the "Driver Score," through the driverDBV3 which incorporates the data from seven computational techniques. DriverDBV3 has been used to examine mutation data focused on one or more specific protein positions, locus enrichment, domains, exons, or cancers.

CONCLUSION

Glioblastoma multiforme (GBM) the most deadly malignant brain tumor still lacks reliable prognostic indicators and therapeutic targets. This work analyzed GBM patient data from cancer databases and clinical biopsy samples of high-grade glioma patients including CNV, MET miRNA, mRNA expression, and clinical information. A total of 20 driver genes, including the following: EGFR, IDH1, PIK3CA, PIK3R1, PTEN, TP53, RHD, LRRC37A,

GSTM1, SIRPB1, SLC24A3, HLA-DRB5, OS9, MELK, ZBTB42, UGT2B17, ENHO, and CDKN2B, were discovered by the ingreation of driver DBV3. Insilico analysis revealed that these 6 genes, EGFR, TP53, PTEN, PIK3CA, PIK3R1, and IDH1, showed mutations in glioblastoma. It is also concluded that TGFB1 is identified with enhanced expression in GBM clinical samples through quantitative analysis may be associated with the presence of mutations .which may promotes invasion, angiogenesis, and the suppression of the immune system in GBM . We anticipate that these mutational analysis of novel driver genes by the application of DriverDBV3 will benefit fundamental research and the development of molecular therapeutics that target their abnormal signalling in GBM.

Institutional Review Board Statement

This retrospective study received approval by the ethical review board of the Capital University of Science and Technology (CUST), Islamabad, Pakistan. All the patients provided verbal and written consent to the scientific use of their data. The biopsy samples of 33 (23 males, 10 females of median age 50 ± 13 years) glioblastoma patients were collected from various surgery departments, public sector tertiary care hospitals of Pakistan who underwent brain surgery between January 2018 and December 2021. Before sample collection, none of the participants in the study had radiotherapeutic or chemotherapeutic treatment.

Informed Consent Statement

Informed consent was obtained from all subjects involved in the study. "Written informed consent has been obtained from the patient(s) to publish this paper" if applicable.

Data Availability Statement

The data presented in this study are available on request from the corresponding authors.

Acknowledgments

We are very thankful to the tertiary care hospitals of Pakistan for helping us in collecting Glioblastoma biopsy samples and the data. Furthermore, we acknowledged Dr Tariq Nadeem for some research experiment performed in cell culture lab, Faculty of life sciences, University of Punjab Lahore Pakistan. We acknowledged Dr Qurban Ali for technical assistance from Institue of agricultural sciences, University of Punjab Lahore Pakistan.

Conflicts of Interest

The authors declare no conflict of interest.

References

1. Khan, F.N., S. Ahmad, and K. Raza, *Clinical applications of next-generation sequence analysis in acute myelogenous leukemia*, in *Translational bioinformatics applications in healthcare*. 2021, CRC Press. p. 41-66.
2. Jensen, M.A., et al., *The NCI Genomic Data Commons as an engine for precision medicine*. Blood, The Journal of the American Society of Hematology, 2017. **130**(4): p. 453-459.
3. Pon, J.R. and M.A. Marra, *Driver and passenger mutations in cancer*. Annual Review of Pathology: Mechanisms of Disease, 2015. **10**: p. 25-50.
4. Jiao, W., et al., *A deep learning system accurately classifies primary and metastatic cancers using passenger mutation patterns*. Nature communications, 2020. **11**(1): p. 728.

5. Gnad, F., et al., *Assessment of computational methods for predicting the effects of missense mutations in human cancers*. BMC genomics, 2013. **14**(3): p. 1-13.
6. Ranjan, P. and P. Das, *Understanding the impact of missense mutations on the structure and function of the EDA gene in X-linked hypohidrotic ectodermal dysplasia: A bioinformatics approach*. Journal of Cellular Biochemistry, 2022. **123**(2): p. 431-449.
7. Kumar, A., et al., *Identifying novel oncogenes: a machine learning approach*. Interdisciplinary Sciences: Computational Life Sciences, 2013. **5**: p. 241-246.
8. Hanif, F., et al., *Glioblastoma multiforme: a review of its epidemiology and pathogenesis through clinical presentation and treatment*. Asian Pacific journal of cancer prevention: APJCP, 2017. **18**(1): p. 3.
9. Suchorska, B., et al., *Identification of time-to-peak on dynamic 18F-FET-PET as a prognostic marker specifically in IDH1/2 mutant diffuse astrocytoma*. Neuro-oncology, 2018. **20**(2): p. 279-288.
10. Rahbari, R., et al., *Timing, rates and spectra of human germline mutation*. Nature genetics, 2016. **48**(2): p. 126-133.
11. Cheng, W.-C., et al., *DriverDB: an exome sequencing database for cancer driver gene identification*. Nucleic acids research, 2014. **42**(D1): p. D1048-D1054.
12. Geeitha, S. and M. Thangamani, *Incorporating EBO-HSIC with SVM for gene selection associated with cervical cancer classification*. Journal of Medical Systems, 2018. **42**: p. 1-10.
13. Liu, S.-H., et al., *DriverDBv3: a multi-omics database for cancer driver gene research*. Nucleic acids research, 2020. **48**(D1): p. D863-D870.
14. Chen, Z. and D. Hambarzumyan, *Immune microenvironment in glioblastoma subtypes*. Frontiers in immunology, 2018. **9**: p. 1004.
15. Deraredj Nadim, W., et al., *MicroRNAs in neurocognitive dysfunctions: new molecular targets for pharmacological treatments?* Current neuropharmacology, 2017. **15**(2): p. 260-275.
16. Nallasamy, P., et al. *PD-L1, inflammation, non-coding RNAs, and neuroblastoma: Immuno-oncology perspective*. in *Seminars in cancer biology*. 2018: Elsevier.
17. Sok, J.C., et al., *Mutant epidermal growth factor receptor (EGFRvIII) contributes to head and neck cancer growth and resistance to EGFR targeting*. Clinical Cancer Research, 2006. **12**(17): p. 5064-5073.
18. Network, C.G.A.R., *Comprehensive genomic characterization defines human glioblastoma genes and core pathways*. Nature, 2008. **455**(7216): p. 1061.
19. Music, D., et al., *Expression and prognostic value of the WEE1 kinase in gliomas*. Journal of neuro-oncology, 2016. **127**: p. 381-389.
20. Munir, H., et al., *Screening a novel six critical gene-based system of diagnostic and prognostic biomarkers in prostate adenocarcinoma patients with different clinical variables*. American Journal of Translational Research, 2022. **14**(6): p. 3658.
21. Sanchez-Vega, F., et al., *Oncogenic signaling pathways in the cancer genome atlas*. Cell, 2018. **173**(2): p. 321-337. e10.
22. Yang, H., et al., *Trans-Driver: a deep learning approach for cancer driver gene discovery with multi-omics data*. bioRxiv, 2022: p. 2022.06. 07.495072.
23. Cui, Y., Y. Zhu, and M. Zhang, *Xinhui Li1†, Jian Zhou2†, Mingming Xiao3†, Lingyu Zhao4†, Yan Zhao5†, Shuoshuo Wang4, Shuangshu Gao4, Yuan Zhuang4, Yi Niu5, Shijun Li6, Xiaobo Li4,*

- Yuanyuan Zhu^{4*}, Minghui Zhang^{5*} and Jing Tang⁴. Omics Data Integration towards Mining of Phenotype Specific Biomarkers in Cancer-Volume II, 2022.
24. Iloshini, P., *Predicting potential cancer driver genes using hybrid approach*. 2021.
 25. Rahimi, M., B. Teimourpour, and S.-A. Marashi, *Cancer driver gene discovery in transcriptional regulatory networks using influence maximization approach*. Computers in Biology and Medicine, 2019. **114**: p. 103362.
 26. Han, Y., et al., *DriverML: a machine learning algorithm for identifying driver genes in cancer sequencing studies*. Nucleic acids research, 2019. **47**(8): p. e45-e45.
 27. Das, T., et al., *Integration of online omics-data resources for cancer research*. Frontiers in Genetics, 2020. **11**: p. 578345.
 28. Herrera-Oropeza, G.E., et al., *Glioblastoma multiforme: a multi-omics analysis of driver genes and tumour heterogeneity*. Interface focus, 2021. **11**(4): p. 20200072.
 29. Carrabba, G., D. Mukhopadhyay, and A. Guha, *Aberrant signalling complexes in GBMs: prognostic and therapeutic implications*. Glioblastoma: Molecular Mechanisms of Pathogenesis and Current Therapeutic Strategies, 2010: p. 95-129.
 30. Crespo, I., et al., *Molecular and genomic alterations in glioblastoma multiforme*. The American journal of pathology, 2015. **185**(7): p. 1820-1833.
 31. Watanabe, K., et al., *Overexpression of the EGF receptor and p53 mutations are mutually exclusive in the evolution of primary and secondary glioblastomas*. Brain pathology, 1996. **6**(3): p. 217-223.
 32. de Souza, C.F., et al., *A distinct DNA methylation shift in a subset of glioma CpG island methylator phenotypes during tumor recurrence*. Cell reports, 2018. **23**(2): p. 637-651.
 33. Thorpe, L.M., H. Yuzugullu, and J.J. Zhao, *PI3K in cancer: divergent roles of isoforms, modes of activation and therapeutic targeting*. Nature Reviews Cancer, 2015. **15**(1): p. 7-24.
 34. Atif, F., S. Yousuf, and D.G. Stein, *Anti-tumor effects of progesterone in human glioblastoma multiforme: role of PI3K/Akt/mTOR signaling*. The Journal of steroid biochemistry and molecular biology, 2015. **146**: p. 62-73.
 35. Koul, D., *PTEN signaling pathways in glioblastoma*. Cancer biology & therapy, 2008. **7**(9): p. 1321-1325.
 36. An, Z., et al., *Epidermal growth factor receptor and EGFRvIII in glioblastoma: signaling pathways and targeted therapies*. Oncogene, 2018. **37**(12): p. 1561-1575.
 37. Nakamura, J.L., *The epidermal growth factor receptor in malignant gliomas: pathogenesis and therapeutic implications*. Expert opinion on therapeutic targets, 2007. **11**(4): p. 463-472.
 38. Endersby, R. and S. Baker, *PTEN signaling in brain: neuropathology and tumorigenesis*. Oncogene, 2008. **27**(41): p. 5416-5430.
 39. Bäcklund, L., et al., *Mutations in Rb1 pathway-related genes are associated with poor prognosis in anaplastic astrocytomas*. British journal of cancer, 2005. **93**(1): p. 124-130.
 40. Wang, X., et al., *Gain of function of mutant TP53 in glioblastoma: prognosis and response to temozolomide*. Annals of surgical oncology, 2014. **21**: p. 1337-1344.
 41. Vegran, F., et al., *Only missense mutations affecting the DNA binding domain of p53 influence outcomes in patients with breast carcinoma*. PloS one, 2013. **8**(1): p. e55103.
 42. Jiang, N., et al., *Role of PI3K/AKT pathway in cancer: the framework of malignant behavior*. Molecular biology reports, 2020. **47**(6): p. 4587-4629.

43. Zhang, M., et al., *Characterization of different oligomeric forms of CRISP2 in the perinuclear theca versus the fibrous tail structures of boar spermatozoa*. *Biology of Reproduction*, 2021. **105**(5): p. 1160-1170.
44. Wang, J., et al., *LncRNA DCST1-AS1 promotes endometrial cancer progression by modulating the MiR-665/HOXB5 and MiR-873-5p/CADM1 pathways*. *Frontiers in oncology*, 2021. **11**: p. 714652.
45. Koch, A., et al., *MEXPRESS: visualizing Expression, DNA methylation and clinical TCGA data*. *BMC genomics*, 2015. **16**: p. 1-6.
46. Joseph, J.V., et al., *TGF- β as a therapeutic target in high grade gliomas—promises and challenges*. *Biochemical pharmacology*, 2013. **85**(4): p. 478-485.
47. Joseph, J.V., et al., *TGF- β promotes microtubule formation in glioblastoma through thrombospondin 1*. *Neuro-oncology*, 2022. **24**(4): p. 541-553.
48. Buonfiglioli, A. and D. Hambarzumyan, *Macrophages and microglia: The cerberus of glioblastoma*. *Acta Neuropathologica Communications*, 2021. **9**(1): p. 1-21.
49. Darmanis, S., et al., *Single-cell RNA-seq analysis of infiltrating neoplastic cells at the migrating front of human glioblastoma*. *Cell reports*, 2017. **21**(5): p. 1399-1410.
50. Vivanco, I., et al., *Differential sensitivity of glioma-versus lung cancer-specific EGFR mutations to EGFR kinase inhibitors*. *Cancer discovery*, 2012. **2**(5): p. 458-471.
51. Shah, V. and J. Shah, *Recent trends in targeting miRNAs for cancer therapy*. *Journal of Pharmacy and Pharmacology*, 2020. **72**(12): p. 1732-1749.